

UCSF

UC San Francisco Previously Published Works

Title

Pathogenic Events in a Nonhuman Primate Model of Oral Poliovirus Infection Leading to Paralytic Poliomyelitis

Permalink

<https://escholarship.org/uc/item/7b17p9sh>

Journal

Journal of Virology, 91(14)

ISSN

0022-538X

Authors

Shen, Ling
Chen, Crystal Y
Huang, Dan
et al.

Publication Date

2017-07-15



DOI

10.1128/jvi.02310-16

Peer reviewed



Pathogenic Events in a Nonhuman Primate Model of Oral Poliovirus Infection Leading to Paralytic Poliomyelitis

Ling Shen,^a Crystal Y. Chen,^a Dan Huang,^a Richard Wang,^a Meihong Zhang,^a Lixia Qian,^a Yanfen Zhu,^a Alvin Zhuoran Zhang,^a Enzhuo Yang,^a Arwa Qaqish,^a  Konstantin Chumakov,^b Diana Kouivaskaia,^b  Marco Vignuzzi,^c Neal Nathanson,^d Andrew J. Macadam,^e Raul Andino,^f Olen Kew,^g Junfa Xu,^a Zheng W. Chen^a

Department of Microbiology and Immunology and Center for Primate Biomedical Research, University of Illinois College of Medicine, Chicago, Illinois, USA^a; Center for Biologics Evaluation and Research, Food and Drug Administration, Silver Spring, Maryland, USA^b; Institut Pasteur, Paris, France^c; Departments of Microbiology and Neurology, University of Pennsylvania School of Medicine, Philadelphia, Pennsylvania, USA^d; National Institute for Biological Standards and Control, Potters Bar, Hertfordshire, United Kingdom^e; University of California San Francisco, San Francisco, California, USA^f; Centers for Disease Control and Prevention, Atlanta, Georgia, USA^g

ABSTRACT Despite a great deal of prior research, the early pathogenic events in natural oral poliovirus infection remain poorly defined. To establish a model for study, we infected 39 macaques by feeding them single high doses of the virulent Mahoney strain of wild type 1 poliovirus. Doses ranging from 10^7 to 10^9 50% tissue culture infective doses (TCID₅₀) consistently infected all the animals, and many monkeys receiving 10^8 or 10^9 TCID₅₀ developed paralysis. There was no apparent difference in the susceptibilities of the three macaque species (rhesus, cynomolgus, and bonnet) used. Virus excretion in stool and nasopharynxes was consistently observed, with occasional viremia, and virus was isolated from tonsils, gut mucosa, and draining lymph nodes. Viral replication proteins were detected in both epithelial and lymphoid cell populations expressing CD155 in the tonsil and intestine, as well as in spinal cord neurons. Necrosis was observed in these three cell types, and viral replication in the tonsil/gut was associated with histopathologic destruction and inflammation. The sustained response of neutralizing antibody correlated temporally with resolution of viremia and termination of virus shedding in oropharynxes and feces. For the first time, this model demonstrates that early in the infectious process, poliovirus replication occurs in both epithelial cells (explaining virus shedding in the gastrointestinal tract) and lymphoid/monocytic cells in tonsils and Peyer's patches (explaining viremia), extending previous studies of poliovirus pathogenesis in humans. Because the model recapitulates human poliovirus infection and poliomyelitis, it can be used to study polio pathogenesis and to assess the efficacy of candidate antiviral drugs and new vaccines.

IMPORTANCE Early pathogenic events of poliovirus infection remain largely undefined, and there is a lack of animal models mimicking natural oral human infection leading to paralytic poliomyelitis. All 39 macaques fed with single high doses ranging from 10^7 to 10^9 TCID₅₀ Mahoney type 1 virus were infected, and many of the monkeys developed paralysis. Virus excretion in stool and nasopharynxes was consistently observed, with occasional viremia; tonsil, mesentery lymph nodes, and intestinal mucosa served as major target sites of viral replication. For the first time, this model demonstrates that early in the infectious process, poliovirus replication occurs in both epithelial cells (explaining virus shedding in the gastrointestinal tract)

Received 28 November 2016 Accepted 8 March 2017

Accepted manuscript posted online 29 March 2017

Citation Shen L, Chen CY, Huang D, Wang R, Zhang M, Qian L, Zhu Y, Zhang AZ, Yang E, Qaqish A, Chumakov K, Kouivaskaia D, Vignuzzi M, Nathanson N, Macadam AJ, Andino R, Kew O, Xu J, Chen ZW. 2017. Pathogenic events in a nonhuman primate model of oral poliovirus infection leading to paralytic poliomyelitis. *J Virol* 91:e02310-16. <https://doi.org/10.1128/JVI.02310-16>.

Editor Julie K. Pfeiffer, University of Texas Southwestern Medical Center

Copyright © 2017 American Society for Microbiology. All Rights Reserved.

Address correspondence to Ling Shen, lshen@uic.edu, or Zheng W. Chen, zchen@uic.edu.

L.S., C.Y.C., and D.H. contributed equally to the article and are co-first authors.

and lymphoid/monocytic cells in tonsils and Peyer's patches (explaining viremia), thereby supplementing historical reconstructions of poliovirus pathogenesis. Because the model recapitulates human poliovirus infection and poliomyelitis, it can be used to study polio pathogenesis, candidate antiviral drugs, and the efficacy of new vaccines.

KEYWORDS oral poliovirus infection, poliomyelitis, animal model, macaques

Although we are approaching the global eradication of circulating wild-type polioviruses, the endgame remains uncertain (1). Wild-type polio cases are still reported in the countries where the virus is endemic, including Nigeria, Afghanistan, and Pakistan (2). Moreover, oral poliovirus vaccine (OPV) immunization with some vaccinees could lead to emergence of circulating vaccine-derived poliovirus (cVDPV), vaccine-associated paralytic poliomyelitis (VAPP), or outbreaks of poliomyelitis (1, 3). Complete cessation of all poliovirus infections requires stopping the use of OPV and developing an improved vaccine and effective drugs to treat chronically infected poliovirus excretors (<http://www.polioeradication.org/ResourceLibrary/Strategyandwork.aspx>). This would involve worldwide transition to inactivated poliovirus vaccines and development of additional prophylactic and therapeutic tools, including antipoliovirus drugs. These development programs are actively supported by the World Health Organization and call for a better understanding of poliovirus pathogenesis, which remains incompletely elucidated (4). Evaluation of these new products would benefit from an animal model that closely resembles human poliovirus infection, and such a model would be of substantial benefit to the global polio eradication endgame.

Mice genetically modified to express the human poliovirus receptor (CD155) are susceptible to parenteral infection with polioviruses. However, they do not adequately model human infection, because they cannot be infected by the natural (oral) route (5–7). Although nonhuman primates (NHP) were historically used for polio research, most studies employed needle injection approaches, rather than single oral exposures, to describe the pathogenesis of poliomyelitis and define vaccine efficacy (4, 8–11). In fact, there has been a lack of in-depth NHP studies using a single oral exposure with tissue-free virus inoculum. Thus, the initial pathogenic events in natural oral poliovirus infection remain poorly defined (4, 9, 12, 13).

Here, we report results aimed at closing this gap by documenting an NHP model that leads to consistent infection with a single dose given by the oral route, followed by a high frequency of paralytic poliomyelitis.

RESULTS

Oral exposure to type 1 poliovirus reproducibly induced productive poliovirus infection in rhesus, cynomolgus, and bonnet macaques. Three species of macaques (rhesus, cynomolgus, and bonnet) were included in the study using the cloned type 1 poliovirus Mahoney. While the poliovirus reproducibly infected CD155⁺ cells and the virus titers in fecal samples could readily be measured by viral plaque assays (Fig. 1a and b), the three species of macaques did not appear to exhibit any significant differences in CD155 expression in peripheral blood lymphocytes (PBL) and gut mucosa (Fig. 1c and d).

A total of 39 macaques were fed single doses (ranging from 10⁹ to 10⁷ 50% tissue culture infective doses [TCID₅₀]) of the highly virulent Mahoney strain of wild type 1 poliovirus contained in 60 ml of apple juice. All the animals were successfully infected, as evidenced by fecal excretion of virus (Fig. 2a and b). Furthermore, 12 of the animals developed overt paralytic disease, with somewhat greater frequency among those fed with the two larger inocula (paralysis rate, 11/29) than among those fed with the lowest inoculum (1/10) (Table 1). The three species of macaques appeared to be equally susceptible, although the small numbers preclude a definitive comparison (Fig. 2a).

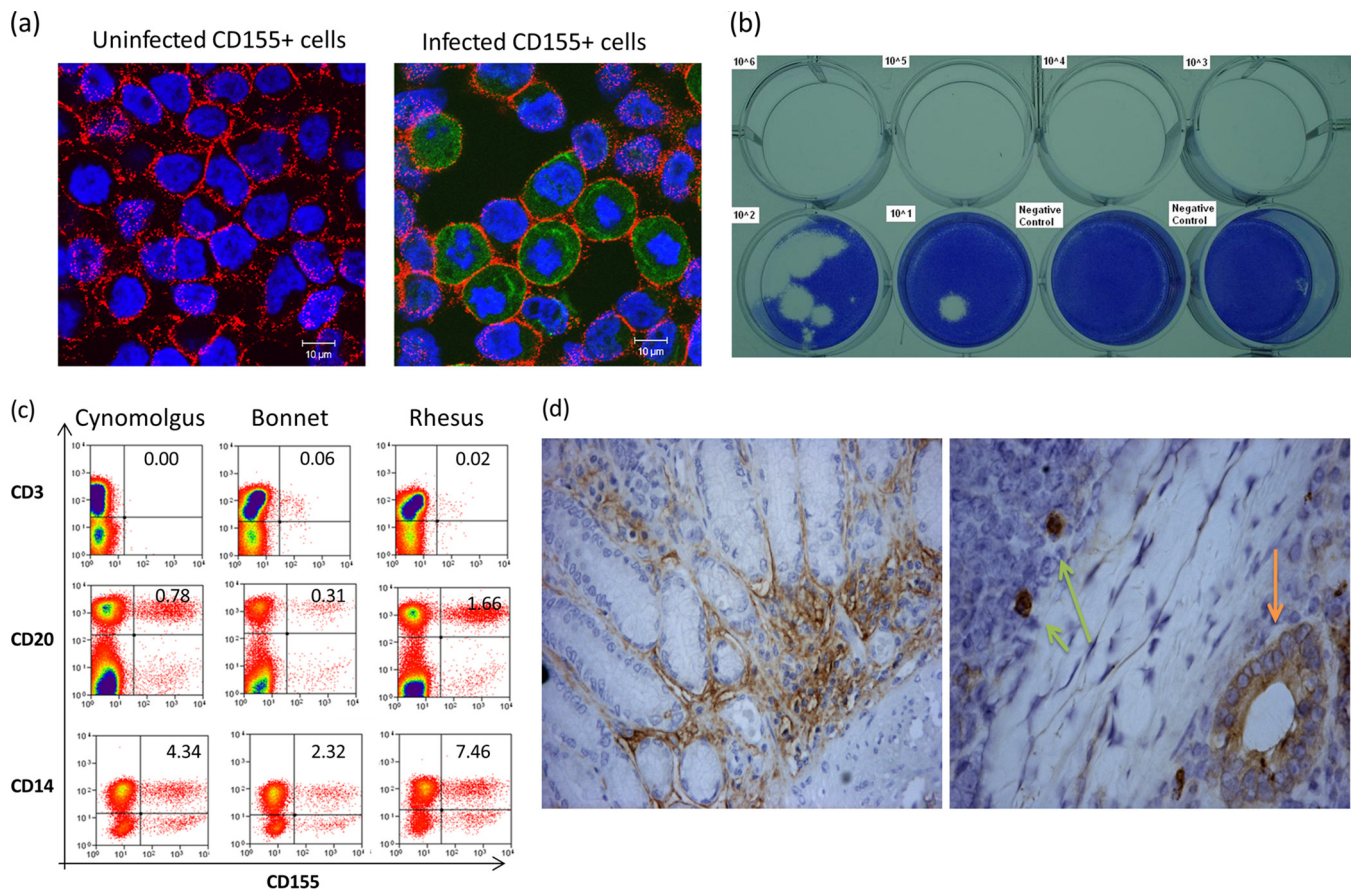


FIG 1 Validation studies of the cloned type 1 poliovirus Mahoney, plaque assay, and CD155 expression in macaques. (a) Representative confocal microscopy images showing that the Mahoney poliovirus reproducibly infected CD155⁺ HeLa cells, as detected by confocal staining of CD155 and type 1 poliovirus protein 1 (VP1). Note intracellular staining of PV1 in green in the infected cells (right), but not the uninfected control (left), after overnight infection with cloned virus (MOI = 100:1) in cultures. There was no staining for isotype controls (data not shown). (b) Representative photograph of PFU assay results. The indicated TCID₅₀ titers of cloned type 1 poliovirus Mahoney were mixed with 50 ml feces from uninfected macaques and then subjected to analysis of PFU counts. Note that approximately 10 TCID₅₀ of cloned poliovirus in feces could form detectable PFU, which served as a detection limit, as well. (c) Representative flow histograms showing that the poliovirus receptor CD155 can be expressed in subsets of CD14⁺ monocytes and CD20⁺ B cells but rarely in CD3⁺ T cells from 3 macaque species (cynomolgus, bonnet, and rhesus). (d) Representative immunohistochemistry analysis of CD155 expression on intestinal mucosal cells of macaques. (Left) Image (magnification, $\times 200$) of CD155 expression on surfaces of intestinal epithelial cells in a tissue section from the small intestine of a representative rhesus macaque. Similar images were seen in the gut sections from other rhesus, cynomolgus, and bonnet macaques. (Right) Image ($\times 400$) of CD155 expression on gut epithelial cells (orange arrow) and cells with macrophage/DC morphology (light-green arrows) in a lymphoid follicle of Peyer's patch in a section from the small intestine of a representative rhesus macaque.

The titers of fecally excreted virus showed a two-phase pattern (Fig. 2b). At day 1 after infection, the inoculum appeared to “pass through” the gastrointestinal (GI) tract, leading to high PFU counts that declined sharply on day 2. Fecal virus increased again on day 3 or day 5 and remained detectable through day 16, while low levels of cytopathic viruses were detected in several animals through day 23. Fecal viruses detected at day 3 or later likely represented replicating poliovirus, based on experiments using neutral red poliovirus (data not shown). Consistent with virus isolation data, a quantitative real-time PCR (qRT-PCR) assay detected high levels of poliovirus RNA in feces from all the animals, confirming the 100% infection rate (Fig. 2b). This sensitive assay turned negative 3 weeks after infection, with no evidence of persistent excretion.

Tonsils, mesentery lymph nodes, and intestinal mucosa served as sites of viral replication after oral infection. We then examined what tissues or sites in the gut contributed to viral replication and fecal shedding after oral feeding of the macaques. Most prior studies were based on virus recovery, and it has not been clear which cells within these tissues actually supported replication (4, 9, 12–14). We presumed that the tissues exhibiting high titers of poliovirus might represent sites of viral replication and

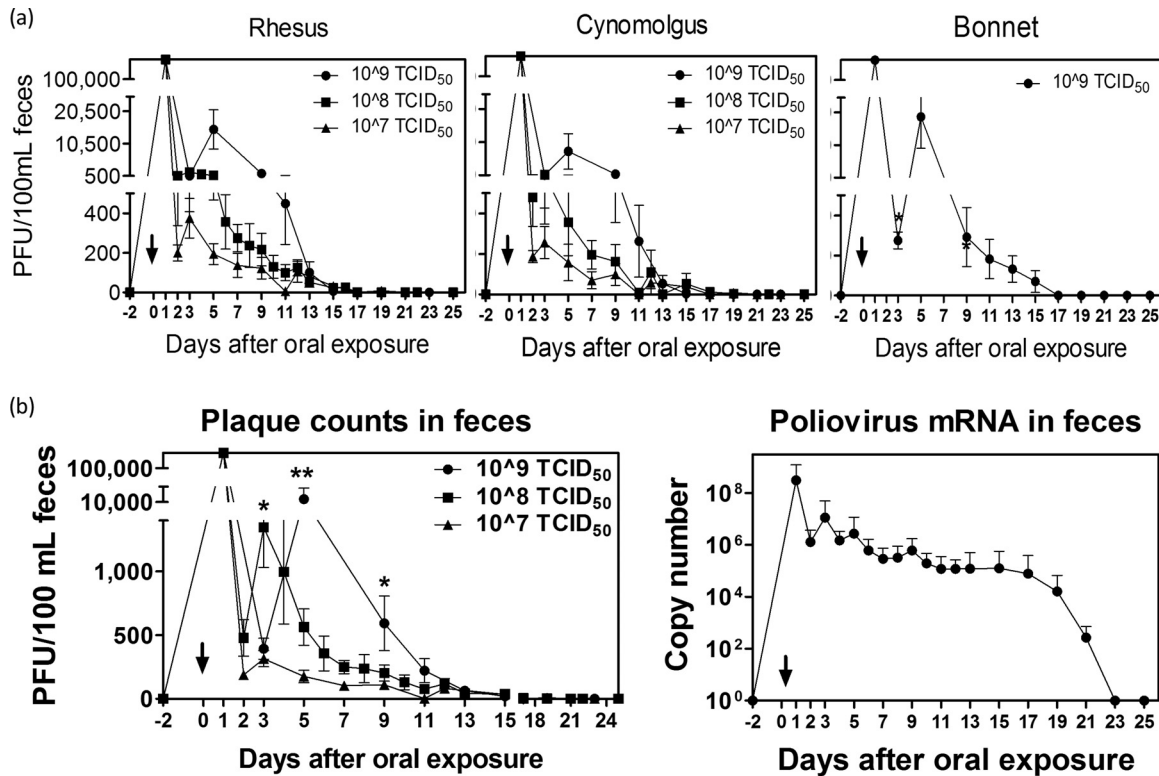


FIG 2 Poliovirus in feces of macaques following oral infection with type 1 poliovirus Mahoney. (a) Mean poliovirus PFU (\pm standard errors of the mean [SEM]) per 100 ml in feces from three different species of macaques following oral infection with 10⁹, 10⁸, or 10⁷ TCID₅₀ Mahoney type 1 poliovirus. The “pass through” virus titers measured at day 1 ranged from 10⁶ to 10⁷, depending upon the feeding dose. *P* values of <0.05 for comparisons between preinfection and days 3 through 13, except day 11, for doses of 10⁹ or 10⁸ TCID₅₀ in rhesus/cynomolgus macaques and except days 11 and 13 for a dose of 10⁷ TCID₅₀. *n* = 21 for rhesus but decreased to 13 from days 8 through 22 due to euthanasia for paralysis; *n* = 15 for cynomolgus but decreased to 12 from days 10 through 22; *n* = 3 for bonnet but decreased to 2 after day 11. (b) Mean (\pm SEM) poliovirus PFU (left) and poliovirus mRNA (right) per 100 ml in feces from NHP fed with 10⁹ TCID₅₀ (*n* = 13), 10⁸ TCID₅₀ (*n* = 16), and 10⁷ TCID₅₀ (*n* = 10) PFU. The data were pooled, since there were no significant differences in patterns between NHP species (panel a). Arrow, infection time; *, *P* < 0.05; **, *P* < 0.01 (between groups).

shedding after oral poliovirus exposure. To test this, we examined tonsils, small and large intestines, and mesenteric lymph nodes from animals sacrificed at days 9 to 12 after oral poliovirus exposure. Polioviruses were measurable in the tonsils and mesenteric nodes, which exhibited higher titers than the small and large intestines (Fig. 3). The quantitative results at the tissue level provided an opportunity to determine what cells were supporting replication and whether the gut epithelium was infected.

Viral replication proteins were detected in both epithelial and lymphoid cell populations expressing CD155 in the tonsil and intestinal mucosa from paralytic monkeys with fecal viral shedding. Next, we sought to determine whether epithelial cells or lymphoid cells harbored poliovirus replication. To date, whether epithelial or lymphoid cells are the primary sites of poliovirus replication in the gut has remained a matter of debate (4, 9). Previously, fluorescence-labeled immunoglobulin from a poliovirus-infected macaque was used to detect poliovirus in epithelia or speculative macrophages after viral feeding (15). Technical difficulties, including nonspecific stain-

TABLE 1 Frequencies of paralysis after oral infection of three species of macaques with three doses of type 1 poliovirus Mahoney

Log ₁₀ inoculum	Rhesus	Cynomolgus	Bonnet	Total
9	2/5	1/5	1/3	4/13
8	5/11	2/5		7/16
7	1/5	0/5		1/10
Totals	8/21	3/15	1/3	12/39

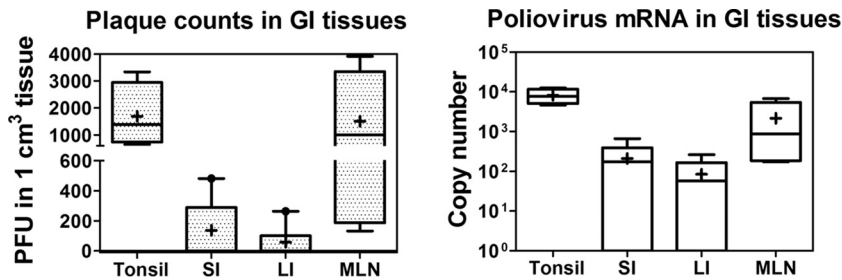


FIG 3 Poliovirus in gastrointestinal tissues of macaques following oral infection with type 1 poliovirus Mahoney. Live poliovirus titers (left) and poliovirus mRNA (copies per milliliter) (right) in homogenates from tonsils, small (SI) and large (LI) intestines, and mesentery lymph nodes (MLN) collected from 8 paralyzed macaques at days 9 to 12 after oral infection with type 1 poliovirus. Boxes and whiskers: the top and bottom hinges represent 90th and 10th percentile values, respectively; +, mean value; horizontal lines in boxes, medians.

ing by the monkey serum (15), indicated a need to conduct a further study. On the other hand, tissue expression patterns for the poliovirus receptor CD155 were compared in humans, macaques, and CD155-transgenic mice, and the presence of CD155 in follicle-associated epithelium and on cells of the Peyer's patches in the gut suggested that they were potentially susceptible to infection (16). However, there is a lack of direct evidence for detecting virus or viral protein in gut epithelia or lymphoid cells in the Peyer's patches after oral poliovirus infection (8, 10, 11, 16, 17).

We employed *in situ* multicolor immune staining of viral replication protein, CD155, and cell markers for epithelium/immune cells in infected tonsils and intestinal mucosa at days 8 to 12 after oral infection of the macaques. Surprisingly, poliovirus polymerase 3D, a surrogate marker for viral replication, was detected in CD155⁺ stratified squamous epithelial cells in the tonsil crypt (Fig. 4a) and CD155⁺ CD11⁺ macrophages/dendritic cells (DC) in the tonsil follicle (Fig. 4b). Similarly, polymerase 3D was also detected in intestinal CD155⁺ epithelial cells (Fig. 4c) and CD11C⁺ macrophages/DC in the intestinal mucosa containing lamina propria or a Peyer's patch-like area (Fig. 4d and e). These results suggest that both epithelial and lymphoid cell populations in oropharyngeal-intestinal mucosae support viral replication and infection after oral exposure in macaques.

Poliovirus infection/replication in the tonsil and gut coincided with histopathologic inflammation and destruction in the epithelia and mucosa-lymphoid interface. Although invasion of intestinal mucosa by poliovirus infection was implicated (13), it has not been reported that poliovirus invasion and replication result in characteristic lesions or destruction of the tonsil and GI mucosa (11, 13, 14, 17). To address this, we conducted thorough histopathology studies of tonsil and gut mucosa harboring high titers of replicating poliovirus, as demonstrated in Fig. 2 to 4. In the Mahoney poliovirus-infected macaques with high virus titers in those tissues, the stratified squamous epithelia lining the tonsil crypts could be disrupted by infiltrating inflammatory cells, with apparent hemorrhage (Fig. 5a top left, arrows). Notably, the destruction and disappearance of the tonsil epithelia coverings were seen (indicated by red arrows in Fig. 5a, bottom left), whereas the crypt lumen was filled with apparent exudates comprised of numerous inflammatory and necrotic cells (red arrows). Similarly, disruptive or necrotic epithelial cells/tissue in the intestinal mucosa was seen, together with inflammatory exudates in the gut lumen and in the lamina propria (Fig. 5b, left). Numerous inflammatory cells were seen to infiltrate the interstitial compartment (lamina propria) or mucosa-lymphoid interface of the small intestine (Fig. 5b, bottom left). Of note, these histopathology changes were not seen in the tonsil and intestinal mucosa from control macaques not infected with Mahoney poliovirus (at Fig. 5a and b, right). Under healthy conditions, new and intact epithelia should be seen to outgrow or replace potentially aging or dying cells without mucosal inflammation or destruction, but this was lacking here. Thus, destruction and histopathologic inflam-

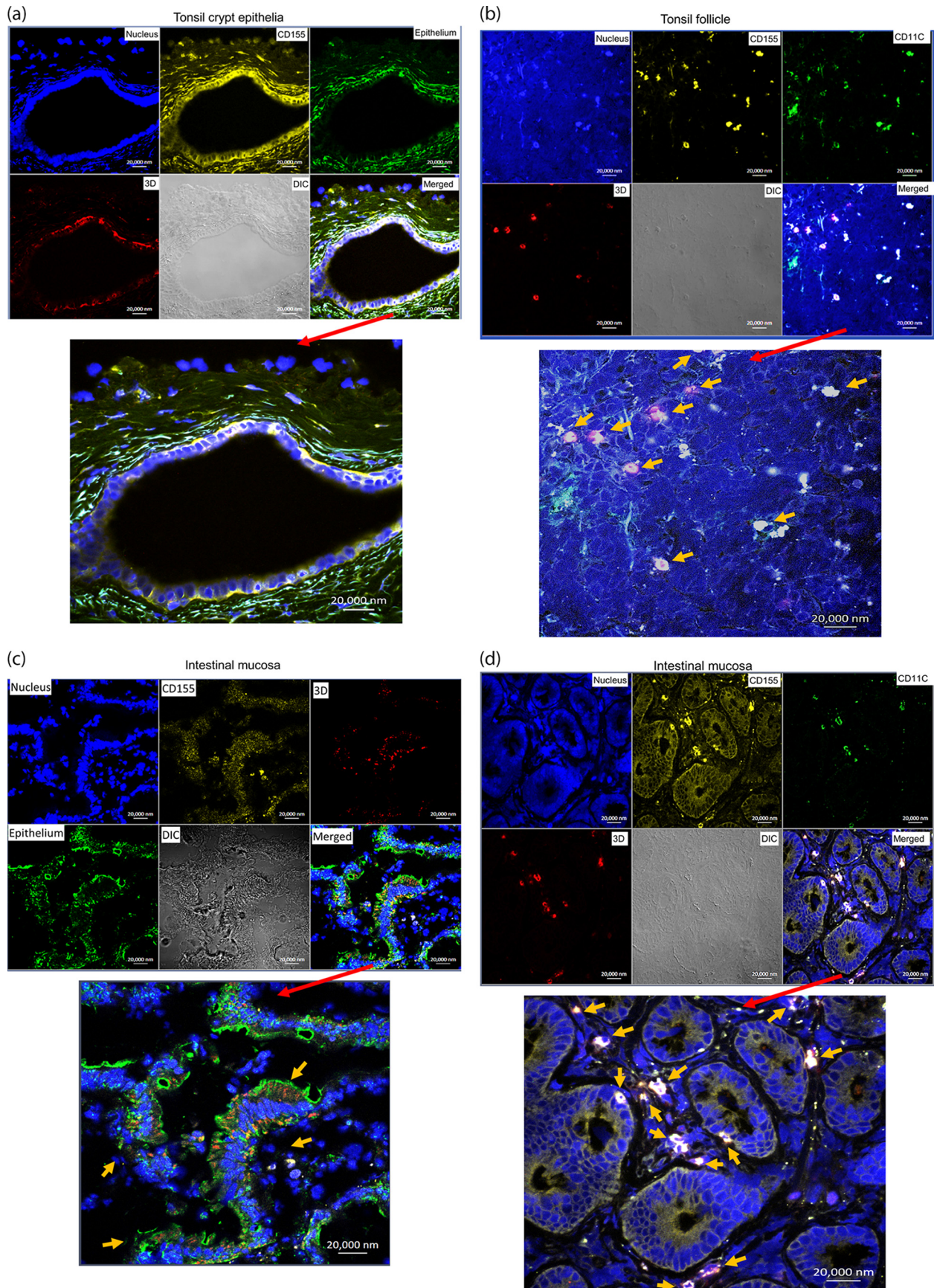


FIG 4 (Continued)

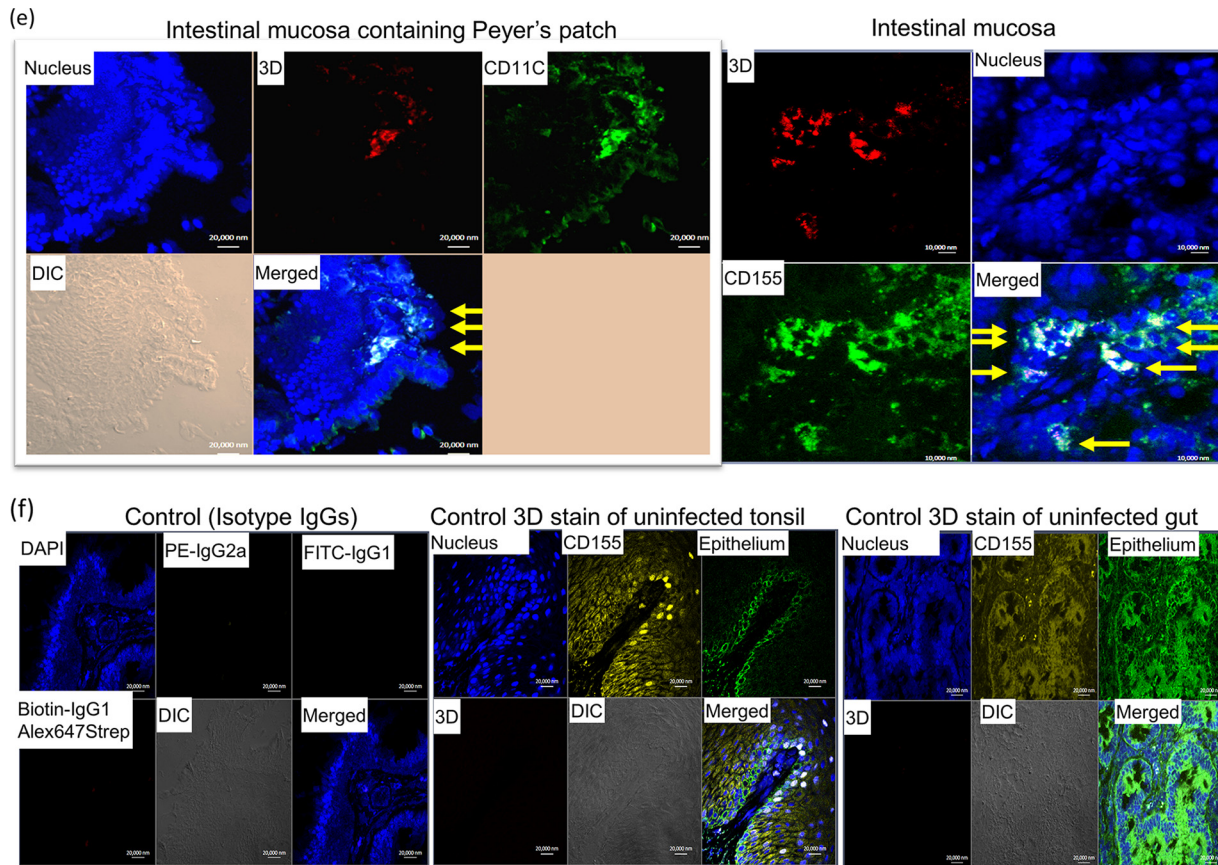


FIG 4 Viral replication proteins were detected in both epithelial and lymphoid cell populations in the tonsil and intestinal mucosa of poliovirus-infected macaques. (a) Poliovirus polymerase 3D was detected in CD155⁺ stratified squamous epithelia lining the tonsil crypt. The merged image is enlarged at the bottom. Note that CD155/epithelial markers overwhelm, but 3D (red) can be judged by referring to the corresponding positions in the multicolor images at the top. DIC, differential interference contrast. (b) 3D was detected in lymphoid cells (CD155⁺ CD11⁺ macrophages/DC) in the tonsil lymphoid follicle. The arrows point to detectable 3D in target cells in the enlarged image. (c) 3D was detected in CD155⁺ epithelial cells in intestinal villi. The arrows point to clustered areas of detectable 3D in epithelia in the enlarged image. Note that epithelia express weaker CD155 than macrophages (center; also see the CD11C⁺ macrophages in panel d). (d) 3D was detected in CD155⁺ CD11⁺ macrophages/DC in the lamina propria of the small intestine. (e) Representative images showing that 3D was detected in CD11C⁺ macrophages/DC in the intestinal mucosa containing the Peyer's patch-like area (left), as well as in CD155⁺ epithelial cells (right, arrows). (f) Representative images showing that control IgG isotypes did not give rise to any staining and anti-3D MAb does not stain tissue sections of tonsil and gut from a healthy macaque not infected with poliovirus. Sections for control isotypes are from intestinal mucosae collected from macaques at days 10 to 12 after oral poliovirus infection, whereas tonsil and small intestine sections for control 3D MAb staining were collected from uninfected macaque RH8335. Shown above are representative images in the sections from the tonsil and intestinal mucosa harboring high titers of replicating poliovirus (Fig. 3). The representative tissues with replicating virus were collected at day 8 or 10 after oral infection of rhesus macaques 8747 and 8745. Poliovirus antigens were detected in tissue sections from five paralyzed rhesus macaques. Fluorescence-labeling Abs and nuclear staining are indicated.

mation in the tonsil and intestinal mucosa are found coincident with detectable viral replication in epithelial and lymphoid cells.

Oral infection with Mahoney poliovirus reproducibly induced acute flaccid paralysis with typical poliomyelitis pathology. As shown in Table 1, 12 of 39 infected animals developed acute flaccid paralysis in the legs and/or arms. The onset of paralysis ranged from 8 to 22 days after oral poliovirus exposure. Eleven of 29 macaques fed with 10^8 or 10^9 TCID₅₀ developed paralysis, whereas only one of 10 macaques fed with 10^7 TCID₅₀ developed paralysis (Table 1).

Eight of 21 rhesus macaques developed paralytic poliomyelitis, and all 8 animals had extensive paralysis involving 3 or 4 limbs. Three of 15 cynomolgus macaques developed paralysis, but two of them had only one paralytic lower limb. The paralyzed macaques were euthanized within 48 h after they developed clinical signs of paralytic poliomyelitis and were subjected to detailed necropsy. Although no gross pathology was found in the central nervous system (CNS), the paralyzed macaques exhibited the

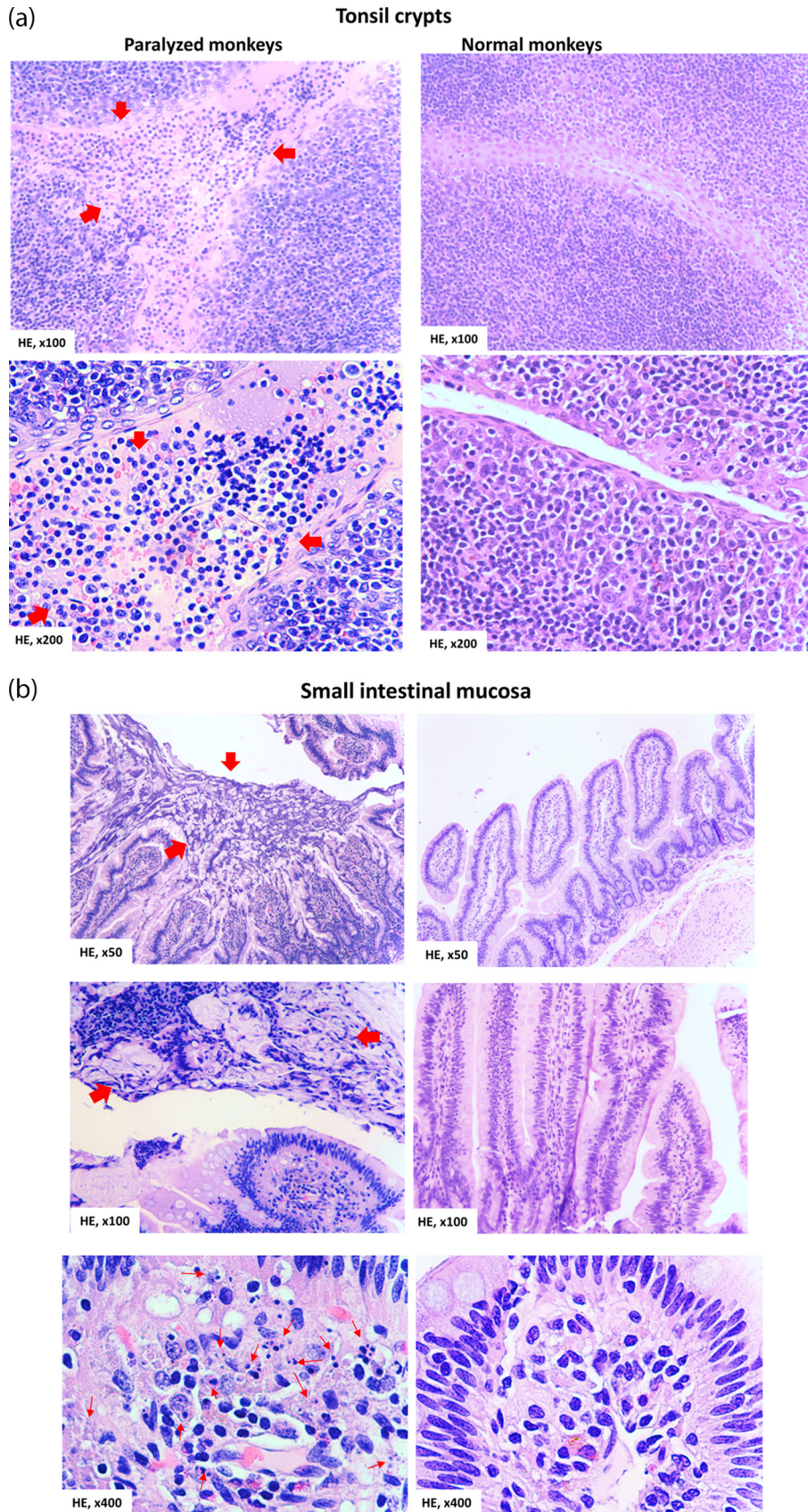


FIG 5 Poliovirus infection in the tonsil and intestinal mucosa coincided with detectable histopathologic lesions and inflammation. (a) (Top left) Representative image showing the hemorrhage and infiltration of
(Continued on next page)

destruction of neurons with neuronophagia, the typical histopathology of poliomyelitis in spinal cord sections (Fig. 6).

Paralytic poliomyelitis after neuronal spread correlated with high titers of poliovirus in the spinal cord and replicating poliovirus in CD155⁺ neurons. CNS tissues collected from monkeys necropsied 24 to 48 h after the onset of paralysis were homogenized and assessed. High titers of plaque-forming polioviruses were detected in the cervical and lumbosacral enlargements and thoracic segments of the spinal cord, while low or moderate titers of poliovirus were found in the brain or brainstem (Fig. 7a, top). High levels of poliovirus mRNA were consistently detected in the same spinal cord homogenates (Fig. 7a). Poliovirus polymerase 3D was detected by confocal microscopy in the cytoplasm of CD155⁺ neurons in the anterior horn sections prepared from the spinal cords of paralyzed macaques (Fig. 7b).

Detectable response of neutralizing Ab correlated temporally with resolution of viremia and virus shedding in oropharynges/stool. The detailed interrelations of neutralizing antibody (Ab) response, viremia, and viral shedding in feces or throats after oral wild-type poliovirus infection leading to paralysis remain incompletely demonstrated in macaques (8, 10, 18). Here, almost all the macaques developed immune responses, as revealed by detection of poliovirus-specific neutralizing Ab starting around 2 weeks postinfection (Fig. 8a). Overall, the neutralizing Ab started to emerge at the late time of transient poliovirus replication in the blood and oropharynges (Fig. 8a and b). Such transient replication was interpreted here by poliovirus-specific qRT-PCR performed on throat washings and peripheral blood mononuclear cells (PBMC), although plaque assay failed to detect plaque-forming live viruses (Fig. 8b). Notably, the neutralizing Ab titers were sustained throughout the experiment, and such sustained responses of neutralizing Abs coincided temporally with resolution of viremia and virus shedding in oropharynges and stool (Fig. 2b and 8).

DISCUSSION

The current study establishes an NHP model for oral infection with human poliovirus that closely mimics natural infection in humans. This study extends previous studies in NHP (8, 10, 12, 13, 16) and helps to fill a longstanding gap in the development of experimental animal models of oral infection leading to development of poliomyelitis. To our knowledge, this work is one of very few studies demonstrating that a single oral exposure to tissue-free poliovirus inoculum is able to induce productive infection and paralytic poliomyelitis in NHP. Historically, in the 1940s, feeding with spinal cord-, feces-, or murine-adapted virus induced a low frequency of paralysis in cynomolgus and rhesus macaques (19–23). Subsequent studies in NHP mostly employed needle injection approaches to confirm human polio and to define vaccine efficacy and the pathogenesis of paralytic poliomyelitis (4, 9, 11). Some studies in the 1950s or later showed that repeated feeding of rhesus or cynomolgus macaques could lead to paralytic consequences (8), but a single oral exposure was unable to induce paralysis

FIG 5 Legend (Continued)

numerous necrotic and inflammatory cells in the stratified squamous epithelia in the tonsil crypt (arrows). (Bottom left) Image showing the destruction and disappearance of the tonsil epithelial covering (red arrows) in the tonsil crypt; the tonsil crypt lumen was filled with hemorrhage and exudates (red arrows) comprised of inflammatory and necrotic cells, including macrophages, neutrophils, and lymphocytes. Of note, new or normal epithelia did not emerge underneath the destroyed tissue (under healthy conditions, new epithelia should be seen to outgrow or replace any potential aging or dying cells). (Right) Histology of undamaged tonsil crypts from control macaques not infected with Mahoney poliovirus. Note the intact structures of the stratified squamous epithelia and clean lumen without inflammatory exudates and cells or hemorrhage. (b) (Top left) Large area of necrotic epithelial cells and tissue (arrows) in the surface of the small intestinal mucosa. (Middle left) Necrotic or destroyed epithelial cells/tissue, together with mucus exudates in the gut lumen (arrows). (Bottom left) Infiltration of numerous inflammatory and necrotic cells (arrows) in the lamina propria in small intestine mucosa. (Right) Intact histology of the small intestine mucosa from control macaques not infected with poliovirus Mahoney. The representative tissue sections were collected from macaques 8745 and 8747, who exhibited high-titer poliovirus and viral replication proteins in the tonsil and intestinal mucosae. Similar histopathologic lesions in the tonsil/intestine could be seen in other macaques infected with poliovirus Mahoney.

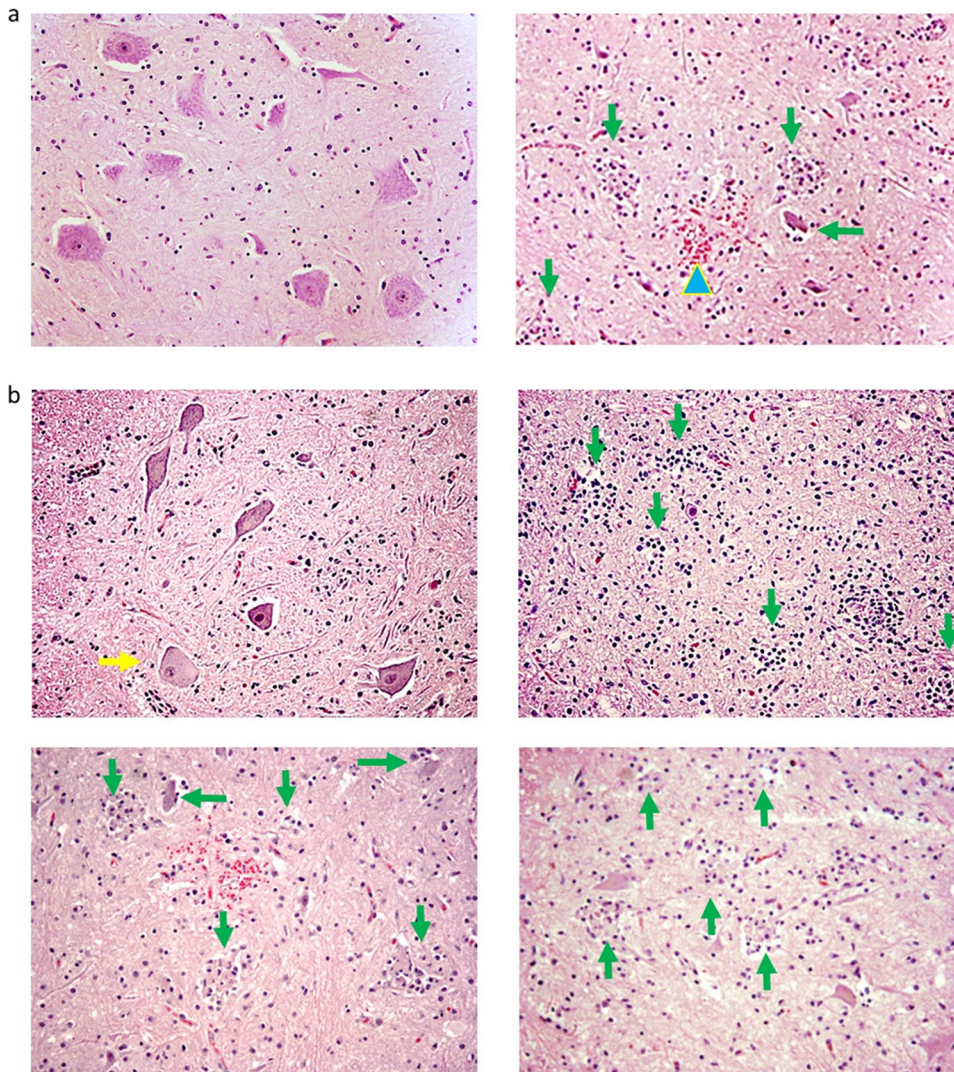


FIG 6 Paralytic poliomyelitis induced by oral poliovirus Mahoney infection was consistent with typical histopathology of poliomyelitis in NHP. (a) (Left) HE-stained section in the left anterior horn of the lumbosacral enlargement from an uninfected healthy control macaque. The section contained spinal motor neurons, astrocytes, and oligodendrocytes. Note the typical appearance of a motor neurons, with a prominent nucleolus in the nucleus and the basophilic Nissl bodies (blue in H&E stain) in the cytoplasm. (Right) Representative H&E-stained section in the lumbosacral enlargement from a paralyzed macaque (RH8203). Note necrotic motor neurons (arrows) and hemorrhage (arrowhead) in the left anterior. (b) (Top left) Section in the left anterior horn of the lumbosacral enlargement from a cynomolgus macaque (CN7821) with paralysis of the right leg. Note that most of the motor neurons in the left anterior horn of the lumbosacral enlargement exhibited “normal” images and only a few degenerative neurons (arrow), with a lack of obvious inflammation and destroyed neurons. (Top right) Section in the right anterior horn of the lumbosacral enlargement from the same cynomolgus macaque (CN7821). Note the completely destroyed neurons, with many neuronophagia (arrows) and infiltration of inflammatory cells. (Bottom left and right) Sections in the left and right anterior horns, respectively, of the lumbosacral enlargement from a rhesus macaque (RH8204) who developed paralysis involving both legs. Note that almost all the neurons in both the left and right anterior horns were destroyed (arrows). RH8203 and the other 2 rhesus macaques with paralysis involving multiple limbs also showed polio lesions in the cerebral cortex and brain stem and the cervical enlargement, respectively (data available upon request).

(10, 22). Our use of large doses of the Mahoney strain, which is known to be highly paralytogenic and pantropic, may explain the 100% infection rate and the surprisingly high frequency of paralysis upon single oral exposure.

Prior studies have claimed that rhesus macaques are resistant to oral poliovirus infection (13, 16) or that repeated oral feeding was needed to induce productive poliovirus infection in rhesus and cynomolgus macaques (8, 21). Our study demonstrated that rhesus macaques were indeed susceptible to productive infection and subsequent paralytic poliomyelitis upon a single oral exposure.

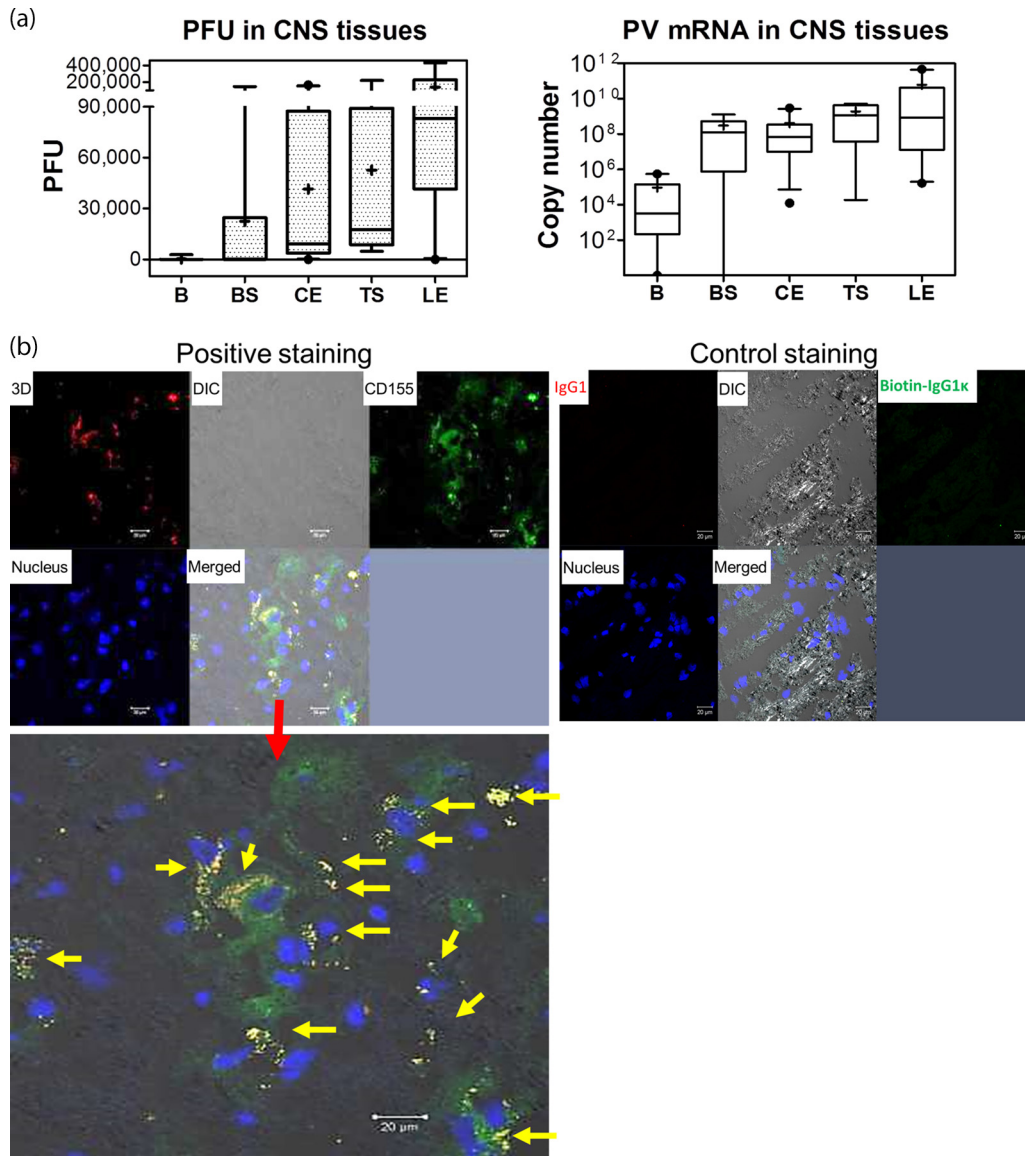


FIG 7 Paralytic poliomyelitis after neuronal spread correlated with high titers of poliovirus in the spinal cord and replicating poliovirus in CD155⁺ neurons. (a) Poliovirus titers (left) and viral mRNA copies (right) per milliliter in homogenates from CNS tissues from 11 paralyzed macaques sacrificed 24 to 48 h after onset of paralysis. The data were pooled, since there were no significant differences in titers between NHP species or between groups fed with different virus doses. The whiskers for the box plots are the same as in Fig. 3. B, brain; BS, brain stem; CE, cervical enlargement of spinal cord; LE, lumbosacral enlargement; TS, thoracic segment. (b) Representative confocal microscopy images showing detection of poliovirus polymerase 3D in CD155⁺ neurons in anterior-horn sections of the spinal cords of paralyzed macaques. (Top left) Representative confocal split images of multicolor staining for poliovirus polymerase 3D (red), CD155 (green), and nucleus (blue) on tissue sections prepared from anterior horns in the lumbosacral enlargement of spinal cord from the rhesus macaque RH8204, who became paralyzed at day 11. (Bottom) Enlarged, merged image showing positively stained poliovirus polymerase 3D in CD155⁺ neurons (arrows) in the anterior-horn sections. Note that the cells harboring 3D are consistent with the sizes of motor neurons, based on the size scale shown. Similar results were seen in other paralyzed macaques. (Top right) There was no staining for isotype IgG controls in spinal cord sections from the paralyzed macaque.

One of our major goals was to establish an oral infection model for studies of polio pathogenesis. We therefore tested 3 high doses to maximize rates of productive infection and paralysis. Using a relatively modest number of macaques, we have achieved our goal of developing a practical oral infection model leading to paralytic poliomyelitis. This success does not support the further use of larger numbers of macaques for a median infectious dose (ID₅₀) or median paralytic dose (PD₅₀) determination.

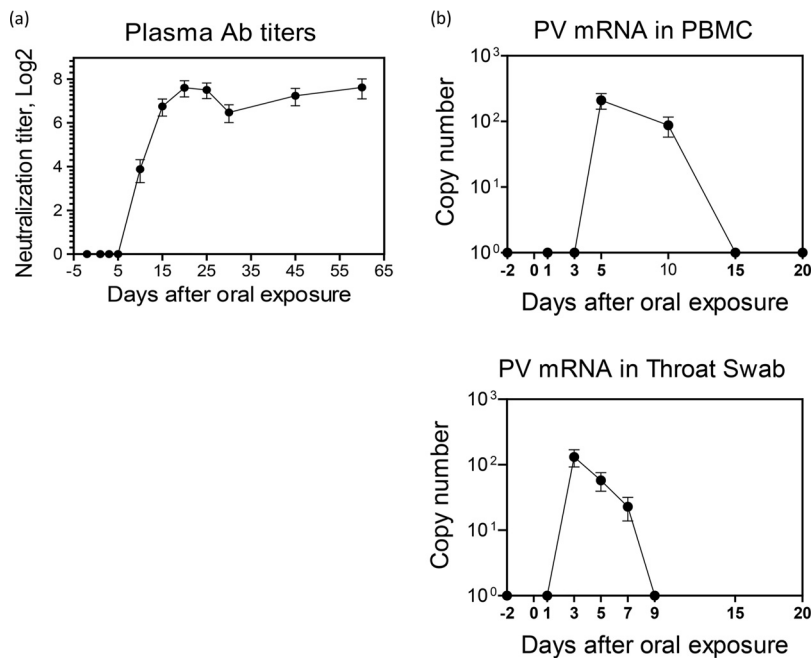


FIG 8 Detectable response of neutralizing Ab coincided temporally with resolution of viremia and virus shedding in oropharynges/stool. (a) Poliovirus-specific neutralization titers (\log_2) after oral poliovirus feeding. Shown are mean dilution titers of plasma with SEM. In geometric scales, log 1 denotes 0. $n = 30$. (b) Poliovirus mRNA copies in blood (top) and throat swab eluate (bottom) from orally infected macaques. The data are mean mRNA copies with standard deviations (SD) in 10^6 PBMC and in 1 ml of throat swab eluate, respectively. Poliovirus mRNA copies in PBMC were pooled from eight macaques who had detectable poliovirus RNA after infection with 10^8 and 10^9 TCID₅₀. None of the macaques infected with 10^7 TCID₅₀ had detectable viral RNA in blood. The data from throat swabs were pooled from 23 macaques. There were no significant differences in frequencies or titers in swabs between species or between the 3 groups infected with 10^7 , 10^8 , and 10^9 TCID₅₀.

It is noteworthy that this highly paralytic model is different from the low paralysis rate in humans. Nevertheless, our model provides an opportunity to dissect polio pathogenesis in the setting of 100% productive infection and high-frequency paralysis after single-dose oral feeding. On the other hand, our data support the presumption that NHP are less sensitive to oral poliovirus infection but more susceptible to paralytic poliomyelitis than humans (13, 24).

In addition to providing a model of “natural” poliovirus infection leading to paralysis, the present study takes the localization of infection from the tissue level to the cellular level, an important advance in understanding the pathogenesis of this infection. We have shown that the virus appears to replicate in stratified squamous epithelial cells in the tonsil crypt and CD11C⁺ macrophages/DC in the tonsil follicle, as well as gut epithelia and macrophages/DC in the small intestine. The results suggest that both epithelial and lymphoid cell populations support viral replication after oral infection, a major extension of the longstanding syntheses proposed by Bodian and Sabin in the 1950s (12, 13). Furthermore, this model also identifies infection-associated histopathologic lesions in the epithelia and mucosa-lymphoid interface of the tonsil and intestine harboring high titers of replicating poliovirus after oral exposure.

In conclusion, the model will be useful for testing candidate antiviral drugs and newly engineered vaccine candidates, which may be required in order to eradicate all poliovirus infections. The model will also enable in-depth mechanistic studies of polio pathogenesis.

MATERIALS AND METHODS

Animals. Thirty-nine macaques, including 21 rhesus macaques (*Macaca mulatta*), 15 cynomolgus macaques (*Macaca fascicularis*), and 3 bonnet macaques (*Macaca radiata*), were used in this study. They

ranged from 3 to 12 years of age and included both females and males, with body weights of 3 to 10 kg. Animal studies were conducted in biosafety level 3 facilities and were approved by the institutional animal care and use committee (IACUC) (ACC15-243).

Oral poliovirus infection. Prior to oral infection, the macaques were trained to voluntarily take apple juice fed via 60-ml catheter-tipped syringes. At the time of single oral feeding, a defined single dose of poliovirus was added to the apple juice for oral administration.

Extraction and concentration of fecal samples from macaques. Feces were collected daily (total excreta, not just a sample) from individual macaques for plaque assays and qRT-PCR. This method was adopted from the protocol provided by Andrew J. Macadam, National Institute for Biological Standards and Control, United Kingdom. Approximately 100 ml of feces from each macaque was divided into five 50-ml high-speed-resistant centrifuge tubes (20 ml each) and mixed with 12 5-mm³ micro-glass beads (Swarovski), 20 ml phosphate-buffered saline (PBS) and 2 ml chloroform. The mixture was shaken on an ice bath by a ProBlot 25× LD Economy Rocker at 120 rpm for 30 min and then was centrifuged at 10,000 rpm for 40 min at 4°C (Avanti J-26XP centrifuge with a JA-12 rotor; Beckman-Coulter). The supernatant was collected and filtered with a Millipore vacuum filtration system. The filtered fecal extracts were transferred into Millipore Amicon 30K centrifugal filter units and contracted by centrifugation at 3,600 rpm for 40 min. This step was repeated to concentrate the extraction into a volume of ~2 ml.

Throat swab eluate preparation. For each animal, a total of 3 sterile polyester-tipped swabs (Puritan) were used to brush against the mucosal surface at the back of the throat, including tonsils and adenoids, and then the swabs were dipped into 1 ml of sterile PBS and vortexed vigorously for 30 s; the swabs were discarded, and the eluate was collected for assays.

Isolation of lymphocytes from blood by Ficoll-Paque. The standard Ficoll-Paque method was described in detail in previous publications (4, 14).

Tissue homogenization. Brain, brain stem, spinal cord (cervical enlargement, thoracic segment, and lumbosacral enlargement), tonsil, small and large intestine mucosa, and mesenteric lymph nodes were collected from the euthanized polio-paralytic macaques. Homogenates were made of 1-cm³ tissue sections, and 5-fold serial dilutions of the homogenate in sterile PBS plus 0.05% Tween were tested by plaque assays and qRT-PCR.

Poliovirus plaque assay. HeLa cells were grown in 12-well culture plates in Dulbecco's modified Eagle's medium (DMEM) with 10% fetal bovine serum (FBS) at 37°C with 5% CO₂ until 90% confluent monolayers (~2 × 10⁶ cells/well) were formed in 24 to 36 h; 100-μl samples were added to each well and incubated at 37°C with 5% CO₂ for 15 min. The cells were overlaid with approximately 2 ml 2% FBS-DMEM agarose gel in each well and incubated at 37°C with 5% CO₂ for 48 h. The gel overlay was gently decanted from each well, and the cell layers were rinsed with PBS, fixed with 1 ml of 2% formalin for 10 min, stained with crystal violet for 10 min, rinsed under water, and air dried. Plaques were counted under a microscope, and titers were expressed as PFU per 100 ml of feces.

Viral RNA isolation and qRT-PCR. Poliovirus RNA was isolated with an RNeasy minikit (Qiagen) and reverse transcribed with a SuperScript III first-strand synthesis system (Life Technologies) following standard protocols from the manufacturer. Sequences of primers were as follows: forward primer, 5'-AGGTCAGATGCTTGAAGC; reverse primer 5'-TCCACTGGCTTCAGTGTT; probe, 5'-CACAGTCCGTGAAA CGGTGG, with 6-carboxyfluorescein (FAM) as the 5' dye and 6-carboxytetramethylrhodamine (TAMRA) as the 3' quencher. The qRT-PCR experiments were performed in an Applied Biosystems 7300 real-time PCR system (Life Technologies), and the PCR products were quantified fluorometrically using TaqMan master mix (Life Technologies), as previously described (25). The qRT-PCR was validated by intra-assays/interassays, with detection limits of RNA copies from ~5 to 10 PFU/100 ml.

In situ confocal microscopic analysis of poliovirus polymerase 3D, CD155, and other markers in tissue sections from poliovirus-infected macaques. The OCT tissue blocks were cut into 6-μm sections using a cryostat, as previously described (26). The frozen tissue sections were fixed with cold acetone for 10 min, rinsed with PBS, and then blocked with protein-blocking serum-free buffer (Dako, X0909) for 30 min. The sections were incubated for 1 h in the dark with diluted primary antibodies (mouse anti-human epithelium monoclonal antibody [MAb], Life Span Bioscience, LS-c65481, or biotin-conjugated mouse anti-CD155 [D171] MAb, GR 224625) in antibody diluent with background-reducing components. The sections were washed twice with PBS and then incubated for 30 min with diluted secondary antibodies (Qdot525 donkey anti-mouse IgG conjugate [H+L], lot 1356566; phycoerythrin [PE]-streptavidin; or fluorescein isothiocyanate [FITC]-streptavidin). Tissue sections were incubated for 30 min with normal mouse serum, washed twice, and then incubated for 30 min with protein-blocking serum-free medium. The sections were then incubated for 1 h with diluted fluorescence-labeled antibodies (allophycocyanin [APC]-conjugated mouse anti-3D MAb, produced/characterized by Gen-Script and the Chen laboratory; phycoerythrin [PE]-conjugated mouse anti-human CD14, BD, catalog no. 555398, or FITC-conjugated anti-human CD11C [Biolegend; catalog no. 301603]). Sections were scanned with a Zeiss LSM 710 confocal microscope using a 40× water objective lens, and images were acquired with the Zen software. Control staining using IgG isotypes or anti-3D staining of normal uninfected tissues did not give rise to fluorescent images on the sections under the confocal microscope (Fig. 4f and 7b).

Gross pathological analysis and histopathologic evaluation of lesions in tonsil and gut as poliomyelitis in the spinal cord. Paralytic animals were euthanized within 24 to 48 h after development of paralysis using intravenous barbiturate overdose and immediately necropsied in a biological safety cabinet. Standard gross pathological evaluation procedures were used. The central nervous system, including brain, brain stem, and spinal cord, and the gastrointestinal tract, including

tonsil, small and large intestines, mesenteric lymph nodes, and other major organs, were collected, examined, and processed for histology analysis. Histopathologic lesions were determined using digital scans to record total pixel counts on hematoxylin and eosin (H&E)-stained sections, and the specimen area was measured in square centimeters using Image-Pro Plus software (Media Cybernetics, Silver Spring, MD), as we previously described (26, 27). Histopathologic lesions in the spinal cord and other CNS tissues were measured in the reference poliomyelitis scores described in the WHO protocol (28).

Microneutralization test. Poliovirus-neutralizing antibody titers were determined in a standard WHO microneutralization test (29).

Statistical analysis. The multivariate analysis of variance (ANOVA) and nonparametric *t* test were used, as previously described (27).

ACKNOWLEDGMENTS

We thank Eun-Chung Park (NIAID) for providing scientific advice, Craig Cameron (Penn State University) for providing 3D antibody, the UIC BRL staff for animal care, Eugenia Dragunsky at the FDA for useful discussion of the histopathology of poliomyelitis, and other staff members in the Chen laboratory for technical support.

This project has been wholly funded with federal funds from the National Institute of Allergy and Infectious Diseases, National Institutes of Health, Department of Health and Human Services, under contract number HHSN266200500016-I (Task Order D23/C28).

We do not have any competing interests.

REFERENCES

- Nathanson N, Kew OM. 2010. From emergence to eradication: the epidemiology of poliomyelitis deconstructed. *Am J Epidemiol* 172: 1213–1229. <https://doi.org/10.1093/aje/kwq320>.
- Roberts L. 2016. Infectious disease. New polio cases in Nigeria spur massive response. *Science* 353:738.
- Hagan JE, Wassilak SG, Craig AS, Tangermann RH, Diop OM, Burns CC, Quddus A, Centers for Disease and Prevention. 2015. Progress toward polio eradication—worldwide, 2014–2015. *MMWR Morb Mortal Wkly Rep* 64:527–531.
- Nathanson N. 2008. The pathogenesis of poliomyelitis: what we don't know. *Adv Virus Res* 71:1–50. [https://doi.org/10.1016/S0065-3527\(08\)00001-8](https://doi.org/10.1016/S0065-3527(08)00001-8).
- Koike S, Horie H, Sato Y, Ise I, Taya C, Nomura T, Yoshioka I, Yonekawa H, Nomoto A. 1993. Poliovirus-sensitive transgenic mice as a new animal model. *Dev Biol Stand* 78:101–107.
- Mendelsohn CL, Wimmer E, Racaniello VR. 1989. Cellular receptor for poliovirus: molecular cloning, nucleotide sequence, and expression of a new member of the immunoglobulin superfamily. *Cell* 56:855–865. [https://doi.org/10.1016/0092-8674\(89\)90690-9](https://doi.org/10.1016/0092-8674(89)90690-9).
- Ren RB, Costantini F, Gorgacz EJ, Lee JJ, Racaniello VR. 1990. Transgenic mice expressing a human poliovirus receptor: a new model for poliomyelitis. *Cell* 63:353–362. [https://doi.org/10.1016/0092-8674\(90\)90168-E](https://doi.org/10.1016/0092-8674(90)90168-E).
- Craig DE, Brown GC. 1959. The relationship between poliomyelitis antibody and virus excretion from the pharynx and anus or orally infected monkeys. *Am J Hyg* 69:1–12.
- Racaniello VR. 2006. One hundred years of poliovirus pathogenesis. *Virology* 344:9–16. <https://doi.org/10.1016/j.virol.2005.09.015>.
- Selvakumar R, John TJ. 1987. Intestinal immunity induced by inactivated poliovirus vaccine. *Vaccine* 5:141–144. [https://doi.org/10.1016/0264-410X\(87\)90062-4](https://doi.org/10.1016/0264-410X(87)90062-4).
- Takahashi Y, Misumi S, Muneoka A, Masuyama M, Tokado H, Fukuzaki K, Takamune N, Shoji S. 2008. Nonhuman primate intestinal villous M-like cells: an effective poliovirus entry site. *Biochem Biophys Res Commun* 368:501–507. <https://doi.org/10.1016/j.bbrc.2008.01.120>.
- Bodian D. 1955. Emerging concept of poliomyelitis infection. *Science* 122:105–108. <https://doi.org/10.1126/science.122.3159.105>.
- Sabin AB. 1956. Pathogenesis of poliomyelitis; reappraisal in the light of new data. *Science* 123:1151–1157. <https://doi.org/10.1126/science.123.3209.1151>.
- Minor PD. 1997. Poliovirus in viral pathogenesis, p 555–574. Lippincott-Raven Publishers, Philadelphia, PA.
- Kanamitsu M, Kasamaki A, Ogawa M, Kasahara S, Imamura M. 1967. Immunofluorescent study on the pathogenesis of oral infection of poliovirus in monkeys. *Jpn Med Sci Biol* 20:175–194. <https://doi.org/10.7883/yoken1952.20.175>.
- Iwasaki A, Welker R, Mueller S, Linehan M, Nomoto A, Wimmer E. 2002. Immunofluorescence analysis of poliovirus receptor expression in Peyer's patches of humans, primates, and CD155 transgenic mice: implications for poliovirus infection. *J Infect Dis* 186:585–592. <https://doi.org/10.1086/342682>.
- Khan S, Toyoda H, Linehan M, Iwasaki A, Nomoto A, Bernhardt G, Cello J, Wimmer E. 2014. Poliomyelitis in transgenic mice expressing CD155 under the control of the TAGE4 promoter after oral and parenteral poliovirus inoculation. *J Gen Virol* 95:1668–1676. <https://doi.org/10.1099/vir.0.064535-0>.
- Selvakumar R, John TJ. 1989. Intestinal immunity to poliovirus develops only after repeated infections in monkeys. *J Med Virol* 27:112–116. <https://doi.org/10.1002/jmv.1890270208>.
- Bodian D, Howe HA. 1945. Non-paralytic poliomyelitis in the chimpanzee. *J Exp Med* 81:255–274. <https://doi.org/10.1084/jem.81.3.255>.
- Horstmann DM. 1952. Poliomyelitis virus in blood of orally infected monkeys and chimpanzees. *Proc Soc Exp Biol Med* 79:417–419. <https://doi.org/10.3181/00379727-79-19398>.
- Horstmann DM, Melnick JL, Ward R, Sa Fleitas MJ. 1947. The susceptibility of infant rhesus monkeys to poliomyelitis virus administered by mouth: a study of the distribution of virus in the tissues of orally infected animals. *J Exp Med* 86:309–323. <https://doi.org/10.1084/jem.86.4.309>.
- Howe HA, Bodian D, Morgan IM. 1950. Subclinical poliomyelitis in the chimpanzee and its relation to alimentary reinfection. *Am J Hyg* 51: 85–108, tab.
- Melnick JL, Von Magnus H. 1948. Comparative susceptibility of cynomolgus and other monkey species to poliomyelitis virus by the intracerebral and oral routes. *Am J Hyg* 48:107–112.
- Knowlson S, Burlison J, Giles E, Fox H, Macadam AJ, Minor PD. 2015. New strains intended for the production of inactivated polio vaccine at low-containment after eradication. *PLoS Pathog* 11:e1005316. <https://doi.org/10.1371/journal.ppat.1005316>.
- Huang D, Qiu L, Wang R, Lai X, Du G, Seghal P, Shen Y, Shao L, Halliday L, Fortman J, Shen L, Letvin NL, Chen ZW. 2007. Immune gene networks of mycobacterial vaccine-elicited cellular responses and immunity. *J Infect Dis* 195:55–69. <https://doi.org/10.1086/509895>.
- Huang D, Chen CY, Ali Z, Shao L, Shen L, Lockman HA, Barnewall RE, Sabourin C, Eestep J, Reichenberg A, Hintz M, Jomaa H, Wang R, Chen ZW. 2009. Antigen-specific Vgamma2Vdelta2 T effector cells confer homeostatic protection against pneumonic plaque lesions. *Proc Natl Acad Sci U S A* 106:7553–7558. <https://doi.org/10.1073/pnas.0811250106>.
- Chen CY, Yao S, Huang D, Wei H, Sicard H, Zeng G, Jomaa H, Larsen MH, Jacobs WR, Jr, Wang R, Letvin N, Shen Y, Qiu L, Shen L, Chen ZW.

2013. Phosphoantigen/IL2 expansion and differentiation of Vgamma2Vdelta2 T cells increase resistance to tuberculosis in non-human primates. *PLoS Pathog* 9:e1003501. <https://doi.org/10.1371/journal.ppat.1003501>.
28. World Health Organization. 25 October 2011. WHO protocol: neurovirulence test of types 1, 2 or 3 live poliomyelitis vaccines (oral) in monkeys. World Health Organization, Geneva, Switzerland. http://www.who.int/biologicals/vaccines/MNVT_protocol_v2510_311011_For_inviting_comments.pdf.
29. World Health Organization. 2004. Polio laboratory manual. World Health Organization, Geneva, Switzerland. http://apps.who.int/iris/bitstream/10665/68762/1/WHO_IVB_04.10.pdf.